

Influence of high temperature treatments under net oxidizing and reducing conditions on the oxygen storage and buffering properties of a $\text{Ce}_{0.68}\text{Zr}_{0.32}\text{O}_2$ mixed oxide

H. Vidal^{b,*}, S. Bernal^a, J. Kašpar^b, M. Pijolat^c, V. Perrichon^d, G. Blanco^a, J.M. Pintado^a, R.T. Baker^a, G. Colon^c, F. Fally^d

^a *Departamento de Ciencia de los Materiales e Ingeniería Metalúrgica y Química Inorgánica, Universidad de Cadiz, Apartado 40, Puerto Real 11510, Spain*

^b *Dipartimento di Scienze Chimiche, Università di Trieste, Via Giorgieri 1, Trieste 34127, Italy*

^c *Ecole Nationale Supérieure des Mines, 158 Cours Fauriel, 42023, Saint Etienne Cedex-2, France*

^d *Laboratoire d'Application de la Chimie à l'Environnement, UMR 5634, CNRS-Université C. Bernard Lyon 1, 43, Bd. Du 11 Novembre 1918, F. 69622 Villeurbanne Cedex, France*

Abstract

TPR, TPO, O_2 pulses and magnetic balance experiments have been performed to study the effect of two different aging treatments, in oxidizing atmosphere and in reducing conditions, on the redox behavior of a $\text{Ce}_{0.68}\text{Zr}_{0.32}\text{O}_2$ mixed oxide.

It has been observed that, although the samples resulting from both treatments have similar textural properties, their redox behavior is significantly different. In particular, aging in H_2 improves the oxygen storage capacity (OSC) at low temperatures by decreasing the temperature at which reduction takes place. Also, the oxygen buffering capacity (OBC) is enhanced after aging under reducing conditions. In addition, the study of the re-oxidation of the samples reveals that the rate of the O_2 uptake increases if compared with the fresh sample or that aged in air. High resolution electron microscopy and Raman spectroscopy data have also been used to obtain information on the possible origin of such effects. ©1999 Elsevier Science B.V. All rights reserved.

Keywords: CeO_2 – ZrO_2 mixed oxides; Oxygen storage capacity (OSC); Oxygen buffering capacity (OBC); TPR/TPO experiments; Magnetic balance; Raman spectroscopy; HREM; Aging treatment; Redox behavior

1. Introduction

For several years, ceria/zirconia mixed oxides have constituted a real alternative to ceria in the formulation of three way catalysts (TWCs) due to their improved redox properties. In particular, they exhibit high OSC, which is related to the occurrence of bulk reduction at a moderate temperature [1]. Moreover, this property

has been found to remain stable even after submitting the oxides to consecutive redox cycles consisting of reduction at high temperature followed by mild re-oxidation [2]. On the other hand, very recently it has been reported that a pre-treatment in an oxidizing atmosphere at high temperature may depress the OSC of these oxides [3]. In summary, the precise origin of these effects is still a matter of discussion and no clear understanding seems to exist yet regarding the influence that different treatments from those already investigated might have on the CeO_2 – ZrO_2 system.

* Corresponding author. Fax: +34-956-834924
E-mail address: hilario.vidal@uca.es (H. Vidal)

The main objective of the present work is to compare the effects on the redox behavior of a ceria–zirconia mixed oxide of two different thermal treatments: one under severe reducing conditions (1223 K) followed by oxidation at moderate temperature (823 K), and a second under oxidizing atmosphere also at very high temperature (1173 K). The oxide investigated was a $\text{Ce}_{0.68}\text{Zr}_{0.32}\text{O}_2$ synthesized in the frame of the so-called CEZIRENCAT¹ project, a research network which benefits from the expertise of nine different labs in several complementary techniques to perform chemical, textural and structural characterization of a series of ceria–zirconia mixed oxides. Recently, we reported the first results obtained in the study of these oxides [3–5].

It is well known that TWCs operate under conditions that fluctuate rapidly between oxidizing and reducing atmosphere. Therefore, to simulate as much as possible the actual operating conditions of these systems, not only the OSC but also the capacity to attenuate quick fluctuations of the oxygen pressure (OBC property [6]) have been analyzed. To our knowledge, no similar approach has been used previously in the literature to investigate the redox behavior of CeO_2 – ZrO_2 mixed oxides.

The close-coupled application of TWCs demands new materials with improved both thermal stability and oxygen storage/release capacity. Thus, the investigation of the textural and structural, and not only chemical effects induced by high temperature treatments under both oxidizing and reducing conditions should be considered as a major objective in the characterization of these materials. In this sense, this work also contributes in an original way to the existing knowledge of ceria–zirconia systems by complementing the chemical information with some data derived from structural characterization. As in Ref. [4], Raman spectroscopy and high resolution electron microscopy (HREM) have been chosen as main techniques for this purpose.

2. Experimental

Three $\text{Ce}_{0.68}\text{Zr}_{0.32}\text{O}_2$ mixed oxides, hereafter referred to as HS, LS and SR oxides were investigated

(compare Table 1). The starting sample (HS) was kindly supplied by Rhodia [4,5]. The LS sample was prepared by heating the HS oxide under wet synthetic air at 1173 K (140 h). The SR oxide was obtained by severe reduction (SR) of the LS sample in flowing H_2 , at 1223 K (5 h) followed by evacuation in a flow of He at 1223 K (1 h) and re-oxidation at 823 K (1 h) in 5% O_2/He .

The textural characterization was performed in a Micromeritics 2100E instrument by using N_2 adsorption/desorption at 77 K and the BET method for the measurement of the specific surface area.

Temperature-programmed reduction (TPR) experiments were carried out in a system equipped with a VG Spectralab SX200 Mass Spectrometer analyser. The amount of catalyst used was 200 mg in all cases. After a standard cleaning pretreatment in 5% O_2/Ar at 823 K (1 h) according to [5], the samples were slowly cooled down to 473 K, and from there to room temperature in pure Ar (20 ml/min). The TPR was then carried out in a flow of 60 ml/min of 5% H_2/Ar at a heating rate of 10 K/min up to a maximum temperature of 1223 K.

The total OSC measurements were performed in a conventional system equipped with a thermal conductivity detector (TCD) as previously described [7], i.e. after reduction at the selected temperature for 1 h, the samples were oxidized by pulsing periodically 0.125 ml of O_2 at 75 s intervals in a flow of Ar at 700 K.

Temperature-programmed oxidation (TPO) was also applied using the same equipment and pulse frequency as in the experiments at 700 K. In this case, each mixed oxide, previously reduced at 1273 K for 1 h, was submitted to pulses of O_2 , first at room temperature (until no more uptake was detected) and then under a heating rate of 5 K/min up to 1273 K. As for the OSC experiments 50 mg of sample was used.

Oxygen buffering capacity (OBC) measurement accounts for the capability to attenuate fast oscillations of oxygen partial pressure. These experiments, whose principles and methodology are described in Ref. [6], consisted of injecting 0.25 ml 5% O_2/He pulses at 10 s intervals into a 60 ml min^{-1} inert gas stream. The O_2 content at the outlet of the reactor was measured by TCD. The O_2 content is the result of the balance of the oxygen injected, consumed and released by the

¹ CEZIRENCAT project is described at <http://www.dschi.univ.trieste.it/cezirencat/index.html>.

Table 1
Textural properties of the Ce_{0.68}Zr_{0.32}O₂ samples

Sample ^a	S _{BET} (m ² /g)	S _t ^b (m ² /g)	Cumulative pore volume (cm ³ /g)	V _{micro} (cm ³ /g)	Average pore diameter (Å)
HS	100	97	0.259	0.001	65
LS	23	15	0.167	0.003	220
SR	19	15	0.174	0.001	220

^a HS: high surface area sample; LS: low surface area samples; SR: severely reduced sample.

^b Surface area determined from the *t*-plot.

sample. The amount of catalyst used in these experiments was 200 mg.

Magnetic susceptibility measurements were carried out with a Faraday micro-balance coupled to a high vacuum system. This technique has proved to be particularly useful in characterizing the redox behavior of ceria-based catalytic materials [8–10]. The experimental set up and the procedure for calculation of the magnetic susceptibilities have been described elsewhere [8,11]. The experiments were performed on 200 mg of mixed oxide placed on quartz wool in a pure silica bucket. All the susceptibility values χ were corrected for the ferromagnetic impurities (<3 ppm Fe or 15 ppm Ni) by plotting χ versus the reciprocal magnetic field and extrapolation to infinite field. They were calculated using cobalt mercurithiocyanate for calibration. The susceptibility of the samples under vacuum after the initial standard pretreatment in 5% O₂/He at 823 K was ca. -0.03×10^{-6} emu cgs g_{oxide}⁻¹ (to be multiplied by 12.56 to obtain SI units in m³ g⁻¹). This value is close to the expected value for a diamagnetic ceria sample containing only Ce⁴⁺ ions. It was taken as a reference corresponding to 0% reduction of the mixed oxide. As in pure ceria, the reduction of ceria/zirconia mixed oxides transforms diamagnetic Ce⁴⁺ into paramagnetic Ce³⁺ species. Thus, the evolution of the magnetic susceptibility as a function of the step by step reduction treatment provides direct information about the changing redox state of the oxide. For each treatment, the extent of reduction was estimated from the susceptibility values obtained at 298 K after cooling the sample under hydrogen and using the value of 11.4×10^{-6} emu cgs g⁻¹ as the susceptibility for pure Ce₂O₃ [12].

Raman spectra were collected on a Perkin–Elmer 2000-FT-Raman spectrometer equipped with a diode-pumped Nd-YAG laser and a room temperature super InGaAs detector. The laser power was 100–500 mW.

HREM images were obtained in a JEOL 2000 EX microscope with a top entry specimen holder and an ion pump and with a structural resolution of 2.1 nm.

3. Results and discussion

3.1. Textural properties

Table 1 summarizes the textural properties of the three mixed oxides. All the samples are mesoporous solids showing only negligible amounts of micropores. The high surface area of the starting HS sample is associated with its appreciable pore volume and relatively small average pore diameter. Both LS and SR sample show remarkably similar textural properties, in spite of different redox behavior (further discussed). The S_{BET} of the HS sample is not correlated with its redox properties (see below). Therefore, the origin of the differences noted must be in the structural rather than in the textural properties.

3.2. Temperature-programmed reduction and OSC measurements

Traces corresponding to the Mass Spectrometer signal 18, which accounts for water evolution from the samples as a consequence of the reduction process occurring during the TPR experiments, are included in Fig. 1. Fresh HS sample features a major peak around 850 K and a minor one around 500 K. The oxidizing treatment leading to the LS sample depresses the reduction at moderate temperature and the main reduction feature is shifted from 850 to 873 K. Note that this treatment decreases the surface area from 100 to 23 m² g⁻¹. Despite a similar loss of surface area the TPR–MS study reveals the enhanced reducibility of the SR sample, as denoted by the shift of the main reduction peak from 850 (HS) to 673 K (SR).

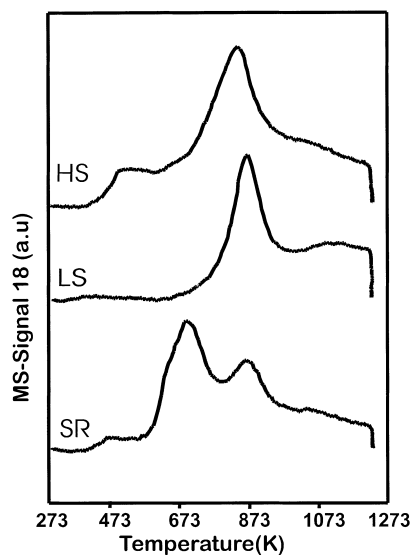


Fig. 1. TPR-MS profiles of the $\text{Ce}_{0.68}\text{Zr}_{0.32}\text{O}_2$ samples.

Table 2

OSC (ml/g) after consecutive reduction treatments (1 h, 5% H_2/Ar) as measured from O_2 pulses experiments at 700 K

T_{red} (K)	HS	LS	SR
473	0.2	0.2	1.5
623	2.0	1.2	6.9
773	9.5	6.7	10.2
973	13.0	9.8	13.4
1173	15.6	13.9	15.3
1273 ^a	16.1	16.1	16.5

^a Separate experiment. Reduction time: 15 min.

The degree of reduction, e.g. the overall oxygen storage was measured as O_2 uptake at 700 K after reduction at different temperatures, and confirms the TPR findings (see Table 2). In fact, consistently with the TPR measurements, and in spite of the relatively low specific surface area of the SR oxide, the improvement of its redox properties in comparison to the starting HS sample is noticeable at temperatures below 773 K. It is noteworthy that the OSC of the SR sample is between three and five times higher than that of the HS and LS oxides after reduction at low temperatures (473 and 623 K). It is also noticed that the LS sample shows lower O_2 uptake over the range of temperatures 473–1173 K compared to the HS sample, which indicates an unfavorable effect of aging under oxidizing

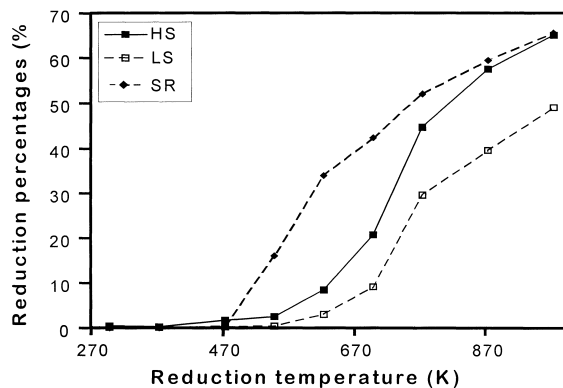


Fig. 2. Reduction percentage $[\text{Ce}^{3+}/\text{Ce}^{3+} + \text{Ce}^{4+} \times 100]$ in the $\text{Ce}_{0.68}\text{Zr}_{0.32}\text{O}_2$ samples obtained from the magnetic susceptibility measurements as a function of the reduction temperature (1 h at each temperature).

conditions. In contrast after the reduction at the highest temperature investigated (1273 K), almost equal OSC is obtained for all the three samples investigated.

3.3. Magnetic balance measurements

Magnetic susceptibility measurements have been carried out to study the Ce^{3+} content in the oxide samples after reduction at different temperatures. For this purpose, after being reduced in flowing 5% H_2/He for 1 h at the selected temperature, the samples were cooled under the same atmosphere down to room temperature. It was verified that reversible hydrogen chemisorption was limited on the mixed oxides to a few percent, ensuring that all the Ce^{3+} present in the samples were associated with the inherent creation of oxygen vacancies [13].

As shown in Fig. 2, a great enhancement of the reducibility is observed for the SR sample, which becomes more reducible than the HS and LS oxides in the whole range of temperatures studied. This is in good agreement with the results obtained by TPR-MS.

3.4. Oxygen buffering capacity (OBC)

The redox properties of these systems under kinetically controlled conditions were investigated by means of the OBC technique [6]. Noticeable differences among the three oxides are found in their ability to buffer fast oscillations of the oxygen partial pres-

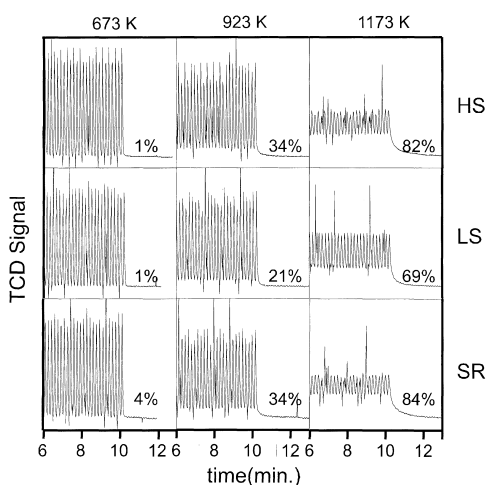


Fig. 3. OBC experiments of the $\text{Ce}_{0.68}\text{Zr}_{0.32}\text{O}_2$ samples at the indicated temperatures. Percentage of attenuation of 0.25 ml 5% O_2/He pulses measured at the indicated temperature is reported. Pulsing frequency: 0.1 Hz.

sure. TCD signals registered during these OBC experiments are plotted in Fig. 3. Remarkably, also under kinetic regime, the different effects of the two aging procedures are clearly evidenced. In fact, in the LS sample a significant deactivation of the oxide is observed (the OBC at 1173 K falls from 81.6% to 69.2%). By contrast, the further high temperature reduction of the LS oxide allows the recovery of the OSC and OBC values, they becoming even better than those of the starting HS sample.

3.5. Kinetics of the O_2 uptake at 700 K/TPO study

The re-oxidation process was investigated by measuring the O_2 uptake at 700 K. The results expressed as cumulative O_2 uptake are reported in Fig. 4. As indicated in Section 2, these data were obtained by injecting O_2 pulses at 700 K over the reduced sample (1273 K, 1 h). All of the samples reach approximately the same overall O_2 uptake, indicating that the cumulative oxygen storage is unaffected by the initial texture of the sample. However, the SR sample shows a linear type of behavior up to complete re-oxidation indicating that every O_2 pulse is completely absorbed until a full re-oxidation is achieved. On the contrary, both HS and LS already show a decreased O_2 uptake after the second pulse, indicating that the kinetics of the O_2

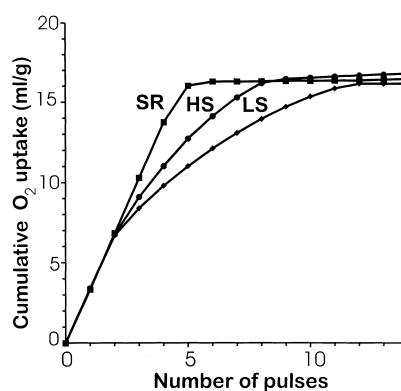


Fig. 4. Cumulative evolution of the O_2 uptake during the pulses experiments carried out at 700 K over the $\text{Ce}_{0.68}\text{Zr}_{0.32}\text{O}_2$ samples reduced at 1273 K for 1 h.

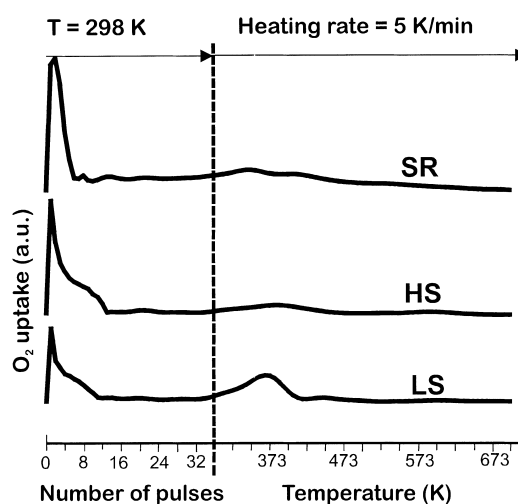


Fig. 5. Pulses at 298 K followed by TPO experiments of the $\text{Ce}_{0.68}\text{Zr}_{0.32}\text{O}_2$ samples reduced at 1273 K for 1 h.

uptake are significantly slower. This is confirmed by the TPO study (Fig. 5). Most of the O_2 uptake already takes place at room temperature, although the complete re-oxidation requires heating up to 373 K. The oxygen pulse experiment at 298 K confirms the faster re-oxidation of the SR sample as denoted by the extra room temperature re-oxidation peak for the HS and LS samples. It should be also noticed that the kinetics of the re-oxidation of the LS sample are remarkably slower compared to the starting HS sample.

In summary the results of the investigation of redox properties clearly show that a high temperature oxi-

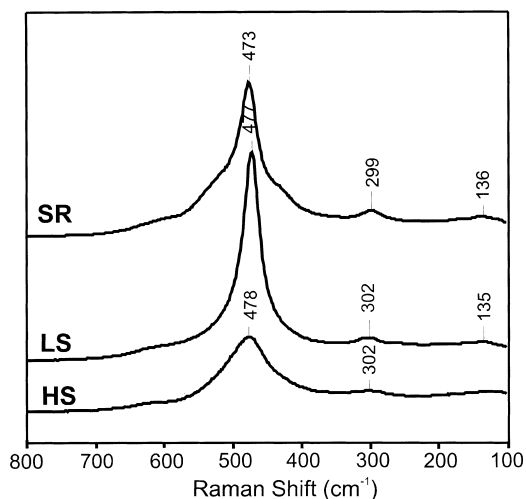


Fig. 6. Raman spectra of the Ce_{0.68}Zr_{0.32}O₂ samples.

dizing pre-treatment strongly depresses the ability of the Ce_{0.68}Zr_{0.32}O₂ mixed oxide to undergo efficient redox processes at low temperature. This effect, however, cannot be attributed to a simple decrease of surface area due to a thermal sintering, since when the same degree of sintering is achieved under a reductive atmosphere, the low temperature redox process is strongly improved compared to the initial HS sample.

3.6. Raman spectroscopy

In order to provide some insight into the origin of these observations, modifications of the oxygen sublattice were investigated by Raman spectroscopy (Fig. 6). There are indeed indications in the literature that modifications of oxygen sublattice induced by the insertion of ZrO₂ into the CeO₂ lattice do occur [14]. All the three samples show a strong band at 473–478 cm⁻¹, which is attributed to the single Raman active mode of *F*_{2g} symmetry allowed for perfect fluorite lattice [15]. However, the presence of weak bands approximately at 300 and 135 cm⁻¹ is an indication of a partial breaking of Fm3m symmetry due to a tetragonal displacement of the oxygen atoms from the tetrahedral sites [16]. Such spectral features are therefore attributed to the presence of a *t'* phase, which is tetragonal phase with the axial ratio *a/c* equal to 1 [16]. There are however some subtle differences in the three spectra. The increase of intensity of the *F*_{2g} mode at

477–478 cm⁻¹ after the oxidative aging is consistent with a sample sintering, which apparently leads to a relatively ordered situation of the oxygen polyhedra around the cations [17,18]. In contrast, the broad *F*_{2g} feature observed in the HS sample suggests a partial breaking of the selection rules due to the small particle size, leading to peak broadening [17]. The same explanation, however, does not hold for the SR sample, which is sintered to the same degree as the LS sample. Accordingly, the broadening of the band at 473 cm⁻¹ in the spectrum of the SR sample is indicative of the breaking of the local symmetry around the cations, suggesting either a high structural disorder in the cubic oxygen sublattice or different geometry of the M–O bonds [14,19]. We suggest that such a phenomenon, which may generate loosely bound — mobile — oxygen atoms in the lattice [14], could be responsible for the improved redox properties of the SR sample.

3.7. High resolution electron microscopy

As a complement to the Raman characterization, the three oxides were also investigated by HREM. Two representative images obtained through this study are reported in Fig. 7. The LS sample shows a typical image of a fluorite type structure as confirmed by the digital diffraction pattern (DDP) obtained from it and reported in the inset. After the severe reduction treatment (SR), a new phase is frequently observed in which at least some of the linear unit cell dimensions double in size as shown in Fig. 7. This could be caused by displacement of O ions from the fluorite positions, ordering of the Ce and Zr cations or both of these in concert. This doubling effect has never been observed in the HS and LS samples. At the present we do not have clear evidence to which extent this phenomenon can be related to the redox properties of the SR sample, however, it should be noted that formation of different CeO₂–ZrO₂ phases under reducing atmosphere has been reported [20,21]. Work is in progress to elucidate this point.

4. Conclusions

1. The effect of high temperature treatment under both oxidizing and reducing conditions

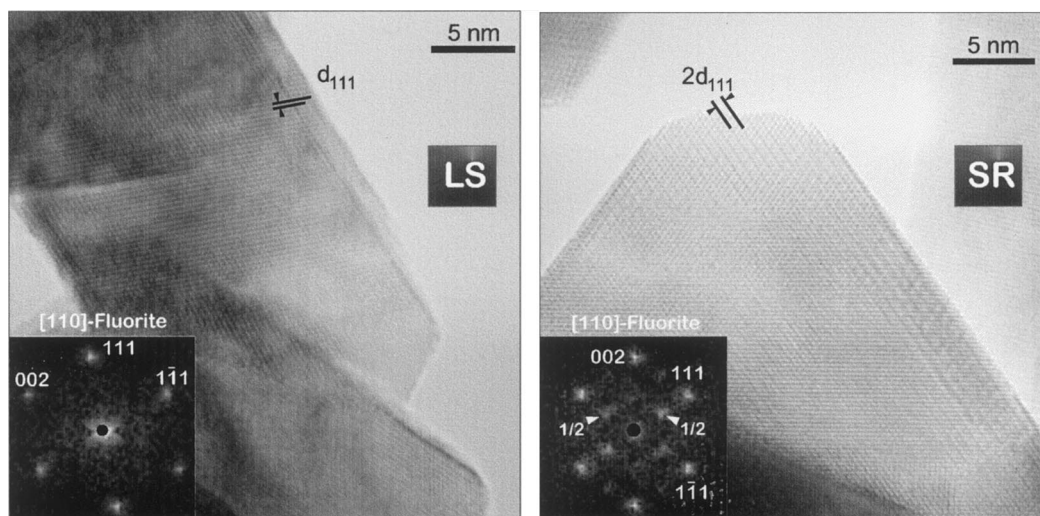


Fig. 7. HREM micrographs of the LS and SR $\text{Ce}_{0.68}\text{Zr}_{0.32}\text{O}_2$ samples with corresponding DDPs inset.

on a $\text{Ce}_{0.68}\text{Zr}_{0.32}\text{O}_2$ oxide sample has been investigated.

2. Aging in air leads to a sample (LS) that shows slow kinetics for both reduction and re-oxidation processes. In contrast a severe reduction treatment leads to an oxide (SR) which presents high capability to both release and take up oxygen, as detected by TPR, TPO, OBC, OSC and magnetic balance experiments.
3. The improvement of the redox behavior of the SR sample compared to the HS and LS is related to the occurrence of redox processes at moderate temperature. Modifications of the oxygen sublattice are suggested to be responsible for this improvement. In contrast, a high temperature reduction (up to 1273 K) leads to an equal degree of reduction, in agreement with a phase stability of these mixed oxides under the present experimental conditions.

Acknowledgements

The present paper has received financial support from the TMR Program of the European Commission (Contract FMRX-CT-96-0060(DG12-BIUO)). H. Vidal, F. Fally, G. Colón and R.T. Baker acknowledge

their fellowships from the TMR Program. The authors also thank Rhodia for providing the HS and LS oxides.

References

- [1] P. Fornasiero, R. Di Monte, G. Ranga Rao, J. Kaspar, S. Meriani, A. Trovarelli, M. Graziani, *J. Catal.* 151 (1995) 168.
- [2] P. Fornasiero, G. Balducci, R. Di Monte, J. Kaspar, V. Sergio, G. Gubitosa, A. Ferrero, M. Graziani, *J. Catal.* 164 (1996) 173.
- [3] R.T. Baker, S. Bernal, G. Blanco, A.M. Cordon, J.M. Pintado, J.M. Rodriguez-Izquierdo, F. Fally, V. Perrichon, *Chem. Commun.*, (1999) 149.
- [4] G. Colon, M. Pijolat, F. Valdivieso, H. Vidal, J. Kaspar, E. Finocchio, M. Daturi, C. Binet, J.C. Lavalley, R.T. Baker, S. Bernal, *J. Chem. Soc. Faraday Trans.* 94 (1998) 3717.
- [5] M. Daturi, C. Binet, J.C. Lavalley, H. Vidal, J. Kaspar, M. Graziani, G. Blanchard, *J. Chim. Phys.* 95 (1998) 2048.
- [6] S. Bernal, G. Blanco, M.A. Cauqui, P. Corchado, J.M. Pintado, J.M. Rodriguez-Izquierdo, *Chem. Commun.* (1997) 1545.
- [7] G. Balducci, P. Fornasiero, R. Di Monte, J. Kaspar, S. Meriani, M. Graziani, *Catal. Lett.* 33 (1995) 193.
- [8] A. Laachir, V. Perrichon, A. Badri, J. Lamotte, E. Catherine, J.C. Lavalley, J. El Fallah, L. Hilaire, F. Le Normand, E. Quemere, N.S. Sauvion, O. Touret, *J. Chem. Soc. Faraday Trans.* 87 (1991) 1601.
- [9] S. Bernal, J.J. Calvino, G.A. Cifredo, A. Laachir, V. Perrichon, J.M. Herrmann, *Langmuir* 10 (1994) 717.
- [10] V. Perrichon, A. Laachir, G. Bergeret, R. Frety, L. Tournayan, O. Touret, *J. Chem. Soc. Faraday Trans.* 90 (1994) 773.

- [11] J.P. Candy, V. Perrichon, *J. Catal.* 89 (1984) 93.
- [12] T. Sata, M. Yoshimura, *J. Ceram. Assoc. Jpn.* 76 (1968) 30.
- [13] S. Bernal, J.J. Calvino, G.A. Cifredo, J.M. Rodriguez-Izquierdo, V. Perrichon, A. Laachir, *J. Catal.* 137 (1992) 1.
- [14] G. Vlaic, P. Fornasiero, S. Geremia, J. Kaspar, M. Graziani, *J. Catal.* 168 (1997) 386.
- [15] V.G. Keramidas, W.B. White, *J. Am. Ceram. Soc.* 57 (1974) 22.
- [16] M. Yashima, H. Arashi, M. Kakihana, M. Yoshimura, *J. Am. Ceram. Soc.* 77 (1994) 1067.
- [17] G.W. Graham, W.H. Weber, C.R. Peters, R.K. Usman, *J. Catal.* 130 (1991) 310.
- [18] W.H. Weber, K.C. Hass, J.R. McBride, *Phys. Rev. B* 48 (1993) 178.
- [19] G. Vlaic, R. Di Monte, P. Fornasiero, E. Fonda, J. Kaspar, M. Graziani, *J. Catal.* 182 (1999) 378.
- [20] S. Otsuka-Yao-Matsuo, N. Izu, T. Omata, K. Ikeda, *J. Electrochem. Soc.* 145 (1998) 1406.
- [21] S. Otsuka-Yao-Matsuo, T. Omata, N. Izu, H. Kishimoto, *J. Solid. State. Chem.* 138 (1998) 47.